

Leveraging Confident Image Regions for Source-Free Domain-Adaptive Object Detection

Mohamed L. Mekhalfi, *Senior Member, IEEE*, Davide Boscaini, Fabio Poiesi

Abstract—Source-free domain-adaptive object detection is an interesting but scarcely addressed topic. It aims at adapting a source-pretrained detector to a distinct target domain without resorting to source data during adaptation. So far, there is no data augmentation scheme tailored to source-free domain-adaptive object detection. To this end, this paper presents a novel data augmentation approach that cuts out target image regions where the detector is confident, augments them along with their respective pseudo-labels, and joins them into a challenging target image to adapt the detector. As the source data is out of reach during adaptation, we implement our approach within a teacher-student learning paradigm to ensure that the model does not collapse during the adaptation procedure. We evaluated our approach on three adaptation benchmarks of traffic scenes, scoring new state-of-the-art on two of them. The code will be released upon acceptance.

Index Terms—Object detection, domain adaptation, cross-domain shift, data augmentation.

I. INTRODUCTION

OBJECT detection is a hot and challenging computer vision topic that benefits many vision tasks [29], [40], [9], [53]. Its challenge stems from several factors such as occlusion, background clutter, and disparity of object appearance [7]. It has animated an exponential growth in the scientific landscape over the past two decades [59]. Source-free domain-adaptive object detection is a research topic that aims at adapting an object detector pretrained on a source dataset to a target dataset drawn from a disjoint distribution, without human labeling. It is relevant in traffic and transportation scenes that are often characterized with dense crowds and vehicles [50], [25].

The progress witnessed in object detection is owed mainly to the advent of deep learning methodologies and the accessibility to pretrained models [21], [45] via transfer learning and opportune fine-tuning, which borrows the knowledge gained by a deep model already pretrained (typically on a large dataset) on an auxiliary task (e.g., image classification) and tailors it to another related task (e.g., object detection) [58], [20]. Ideally, this would require target ground-truth for optimal transferability. In real scenarios, however, this is not necessarily guaranteed, which may constitute generalization bottlenecks for data-hungry deep learning paradigms. In this respect, domain adaptation (DA) has emerged as a potential

remedy [33], [24], [26]. Essentially, it aims at leveraging the knowledge learned by a model on annotated source data (also referred to as source domain/distribution), in order to adapt the model to a target domain that lacks or has partial annotation (i.e., unsupervised, few-shot, or semi-supervised) [33]. Unlike the fairly straightforward transfer learning, DA typically requires building specific methodologies for the adaptation problem at hand. Precisely, DA comes at the expense of distribution mismatch across domains (source vs target), which can be due to weather changes [44], [54], acquisition time (e.g., daytime vs nighttime) [23], nature of data (e.g., synthetic vs real) [34], locations (e.g., different cities) [15], and camera (e.g., RGB vs thermal) [49].

Relevant research on DA for object detection suggests several settings. Unsupervised DA (UDA) for object detection represents the majority of contributions [33]. It proceeds by pretraining a base detector on a source domain, and then adapts it on the target images involving the source data again to maintain the model’s knowledge gained on the source and prevent eventual collapse (i.e., catastrophic forgetting [1]). However, real-life cases imply different situations because source data may not be granted due to (for instance) privacy concerns [4], [14]. This gave rise to an extreme variant of UDA, namely source-free UDA (SF-UDA), where only the target domain images are accessible at the adaptation phase of the already source-pretrained detector. Hence, it poses major challenges due to the lack of source groundtruth.

Compared to UDA, SF-UDA is far less addressed in the relevant literature, and there is plenty of room for improvement. Data augmentation paradigms have been shown to be useful in image classification, object detection and segmentation purposes [8], [2], [51], [22], [13]. They offer the advantage of manipulating the input images/labels without altering the model’s architecture. Although data augmentation was addressed (at least scarcely) in the UDA setting, to our awareness it was not leveraged in the SF-UDA scenario. To this end, this paper devises a novel data-augmentation based approach for SF-UDA, namely SF-DACA which stands for *source-free detect, augment, compose, adapt*, indicating four sequential steps that the adaptation process undergoes. SF-DACA capitalizes on the knowledge learned from the source domain during the pretraining phase to derive high quality predictions from the target domain, and further treat them as pseudo-labels to increment the knowledge on the target domain. This is achieved by selecting confident target image regions and their respective pseudo-labels and joining them via augmentations into one image to self-train the detector. Because the detector does not possess knowledge on the target, pseudo-labels often comprise false positives, which if

Corresponding author: M. L. Mekhalfi (email: mmekhalfi@fbk.eu). M. L. Mekhalfi, D. Boscaini, F. Poiesi are with Fondazione Bruno Kessler (FBK), 38123 Trento, Italy. This paper is supported by European Union’s Horizon Europe research and innovation programme under grant agreement No 101092043, project AGILEHAND (Smart Grading, Handling and Packaging Solutions for Soft and Deformable Products in Agile and Reconfigurable Lines).

augmented as explained earlier, will grow and mislead the adaptation process if the knowledge on the source domain is not maintained, ultimately causing a collapse as evidenced experimentally in Sec. IV. To cope with this, a teacher-student approach is proposed in this paper, where both the teacher and the student models are initially pretrained on the source domain. During adaptation, the dynamic student is adapted towards the target via the four aforementioned steps. Simultaneously, the student’s knowledge is maintained through a consistency loss against the predictions of the static teacher on the target images. We increment the teacher knowledge on the target by partially inheriting student weights using exponential moving average [48].

This paper is an extension of our prior work, DACA [31], in several aspects. First, we surveyed more related works, and we summarized a comprehensive table that reports key-features, and the setup of different works. Second, we extended DACA [31] from UDA to the SF-UDA setting. To our knowledge, SF-DACA is the first approach that exploits data augmentation in the SF-UDA scenario. Third, we extended the experimental validation and we achieved superior results w.r.t to prior works.

The rest of the paper is organized as follows. Sec. II reviews existing relevant art. Sec. III describes the proposed SF-DACA. Sec. IV conducts the experiments and their discussions. Sec. V wraps up the paper.

II. RELATED WORKS

A. Object detection

Existing works can be categorized into two-stage or one-stage detectors. Regarding the former one, regions with CNN (R-CNN) features [12] introduced impressive performance. Fast R-CNN [11] passes the entire image through the CNN once, making inference much faster. Faster R-CNN [36] integrates region proposal networks to predict region proposals that require only negligible additional computation.

As per the one-stage detectors, they seek to abandon the proposals step, and directly predict the bounding boxes and class labels for objects in one pass. For instance, single shot multibox detector (SSD) [28] produces a fixed set of default bounding boxes and predicts the class label and the bounding box coordinates for each one. You Only Look Once (YOLO) [35] divides the image into an even grid, where each grid is responsible for detecting objects whose center falls within it, drastically reducing the processing overheads. YOLO has evolved into several versions, a chronological narrative was conducted in [43]. RetinaNet [39] addresses the class imbalance via a Focal Loss that focuses training on a sparse set of hard examples and prevents the vast number of easy samples from overwhelming the detector [39]. CenterNet [56] assumes that each pixel in a predicted heatmap stands for a keypoint that represents the center of a potential object in the input image, and regresses to all other object properties. In [3], an encoder-decoder detection transformer that predicts all objects at once was presented. EfficientDet [47] combines EfficientNet backbone for feature extraction, and a bi-directional feature pyramid network for efficient feature fusion.

B. Unsupervised domain adaptation for object detection

UDA setting is the most addressed in the literature. Various schemes have emerged so far, such as style transfer, feature alignment, and self-training (see the first part of Tab. I).

Style transfer methods attempt to mitigate the domain shift at image level by modifying the appearance of source images to make them similar to target images, thus improving the generalization of an object detector on the target domain. Rodriguez et al. [38] adopt a feed-forward stylization method proposed in [18]. A curriculum approach was presented in [46], by opting for Cycle-GAN for the styling task, which enables the detector to adapt towards the target domain in a progressive way from easy to hard samples. The pipeline developed in [52] manipulates the receptive field of Cycle-GAN to pay more attention to low-level style cues such as object details and its immediate context. Munir et al. [32] also argue that low-level features work well when styling source images from the visible spectrum to target images from the infrared spectrum. A bidirectional styling approach was proposed in [55] by incorporating source-like target images and target-like source images into a student-teacher learning framework. In this regard, style transfer is a straightforward technique to alleviate domain discrepancy. However, it remains limited in scenarios where a distribution shift occurs within the source and/or the target domains themselves, in which case style transfer may imitate cross-domain style partially.

Feature alignment approaches go beyond image-level and reason at feature-level instead. Adversarial training is the most frequent approach. So far, there is no consensus whether global or local feature alignment works best. In [57], regions of interest (e.g., region proposals derived from a Faster-RCNN) are mined and their respective feature representations are subsequently aligned in an adversarial manner. Motivated by the fact that image-level feature alignment leads to noisy foreground-background alignment, and that instance-level alignment often involves background signals, the method in [16] pays more attention to foreground pixels with higher objectness and centerness scores (these latter two are inferred from objectness and centerness maps via a fully-convolutional module). Other methods combine both style transfer and feature alignment such as [17], where source images are translated to target style using a CycleGAN, then the intermediate stylized domain image features are aligned with the target features via adversarial learning. In [37], instance proposals (Faster R-CNN) are first aggregated based on visual similarity into class-agnostic feature clusters via hierarchical agglomerative clustering.

Pseudo-label self-training is another approach that mines confident detections from the target images and uses them as supervision to adapt the detector. In SC-UDA [52], multiple detections from the target are obtained by implementing a stochastic dropout into the detector’s feature extraction layers during both training and testing phases. The detections with higher IoUs are then fused and leveraged to self-adapt the detector. Confident pseudo-labels combined with hard augmentations are used to self-train the detector in [41]. ConfMix [30] selects the most confident region in the target image and pastes it into the source image, which is redundant

because the detector is already supervised with consistency loss on the source data during adaptation. DACA [31] tackles this downside. Instead of mixing the confident target region with a source image, DACA augments it randomly (along with the pseudo-labels therein) to produce challenging regions and then joins these latter into a final image that can be used to adapt the detector. Therefore, DACA does not mix cross-domain images but instead composes informative target images to adapt the detector.

C. Source-free unsupervised domain adaptation for object detection

SF-UDA has attracted far less attention w.r.t UDA. Most existing works in this setting opt for a teacher-student learning paradigm (see the second part of Tab. I). For instance, in [50] an auxiliary target domain is created by perturbing target images. Then the target and the auxiliary target images are fed to the teacher and student models (both pretrained on the source domain). The student model admits region proposals (i.e., Faster R-CNN) from the teacher model, and is trained with three consistency losses, namely image-level, instance-level, and category-level. LODS [25] adopts a similar concept by generating an auxiliary target domain via target image style enhancement. This is achieved through a non-linear combination of the input target image and any other target image (i.e., fully connected layers and a ReLU applied on the image features derived by a pretrained VGG-16 model). ASFOD [5] argues that the source-pretrained detector tends to infer more predictions on hard target images that exhibit similarity to the source domain, while ignoring hard target images that are dissimilar to the source, yet they manifest high uncertainty, and score high variance during adaptation. Intuitively, the target domain is divided accordingly into source-similar and source-dissimilar subsets. Next, a student-teacher flow is adopted to align these two subsets in an adversarial learning. Finally, a mean-teacher step is achieved to finetune the detector. LPU [4] imposes two confidence thresholds on the pseudo-labels generated by the teacher model, namely a high threshold and a low threshold. For the detections exceeding the high threshold, traditional mean-teacher framework is invoked. As per the pseudo-labels exceeding the low threshold and below the high threshold, proposal soft training is carried out by feeding the (Faster-RCNN) proposals to the teacher model to obtain class predictions, which are then leveraged to self-train the student model with its own proposals. Moreover, an IoU-mixup is conducted on the proposals in the spatial location neighborhood, to make the model aware of the relationship between neighboring proposals via contrastive learning. SFOD-Mosaic [26] employs self-training with pseudo-labels to adapt towards the target. It assumes that the noise degree of the pseudo-detections is positively correlated with the mean self-entropy, indicating a potential to measure the predictions uncertainty. Thus, positive and negative target samples are distinguished by searching for a confidence threshold from the higher to the lower scores, and self-entropy descent is observed when the mean self-entropy descends and hits the first local minimum, and adapts the detector accordingly.

III. OUR METHOD

A. Overview

Suppose a labeled source domain $D_s = \{(x_s^i, y_s^i)\}_{i=1}^{N_s}$ and an unlabeled target domain $D_t = \{x_t^i\}_{i=1}^{N_t}$ that obey disjoint distributions, where $x_s^i \in \mathbb{R}^{H \times W \times 3}$ and $x_t^i \in \mathbb{R}^{H \times W \times 3}$ are RGB images randomly sampled from the source and target domains respectively, and $y_s^i = (b_s^i \in \mathbb{R}^{M_s \times 4}, c_s^i \in \mathbb{N}^{M_s \times 1})_{i=1}^{N_s}$ denotes the groundtruth bounding box coordinates and categories of the objects included in the image x_s , where M_s is the number of objects, and C is the number of object classes. An object detection model can be defined as a parametric function $\Phi_\Theta: \mathbb{R}^{H \times W \times 3} \rightarrow \mathbb{R}^{M \times 4} \times [1, \dots, C]^M$ with learnable parameters Θ that admits an RGB image x as input and infers a list of M detections.

The aim in classical UDA is to adapt an object detector that was pretrained on the source domain D_s to the target domain D_t , while having access to the source data in D_s during adaptation, which helps prevent catastrophic forgetting. In SF-UDA, the source data is unavailable, and the source-pretrained detector is adapted with target images $D_t = \{x_t^i\}_{i=1}^{N_t}$ only.

In order to cope with potential model collapse due to the lack of source data, in this paper we develop a student-teacher learning approach that assumes two source-pretrained models that have identical architectures, namely a teacher detector parameterized with Θ_{tea} and a student model parameterized with Θ_{stu} . The role of Θ_{stu} is to adapt towards D_t , while the role of Θ_{tea} is to prevent Θ_{stu} from collapsing.

B. Self-training with regional pseudo-labels

The proposed SF-DACA takes advantage of self-training to approach the target domain. This indicates the mining of pseudo-labels from the target images and utilizing them as groundtruth to finetune the detector on the target. Yet, we argue that these pseudolabels should be (i) reliable, (ii) convey spatial context, and (iii) informative/challenging. The reliability implies that the detector is adapted with pseudo-labels that correspond to actual objects of interest, and the spatial context enables the detector to perceive the visual aspect of objects among other objects/background, while the informative/challenging property prevents the detector from overfitting the target images.

To tackle all these three key properties, we propose to adapt the student model $\Phi_{\Theta_{\text{stu}}}$ with composite target images that are formed by leveraging regional pseudo-labels. To this end, given a randomly sampled target image x_t , we feed it to the student model Θ_{stu} to infer a set of M_{stu} detections $y_{\text{stu}} = (b_{\text{stu}} \in \mathbb{R}^{M_{\text{stu}} \times 4}, c_{\text{stu}} \in \mathbb{N}^{M_{\text{stu}} \times 1}, p_{\text{stu}} \in \mathbb{R}^{M_{\text{stu}} \times 1})$, where p_{stu} is the detection confidence. First, to make use of reliable pseudo-labels with visual context, we divide the target image x_t into four spatial regions $r_{tl}, r_{tr}, r_{bl}, r_{br}$, which respectively stand for the top left, top right, bottom left, and bottom right image regions that constitute the whole target image $x_t = r_{tl} \cup r_{tr} \cup r_{bl} \cup r_{br}$.

Next, we select the most confident image region based on the average detection confidence in that image portion $p_r = \frac{1}{n_r} \sum_{i=1}^{n_r} p_i$ where n_r is the number of regional detections and p_i are their respective confidences. In particular, in each

TABLE I

OVERVIEW OF EXISTING UDA AND SF-UDA APPROACHES. THE FOLLOWING NOTATIONS ARE USED IN THE TABLE, NAMELY SOURCE: SOURCE DATASET, TARGET: TARGET DATASET, C: CITYSCAPES, F: FOGGYCITYSCAPES, K: KITTI, S: SIM10K, P: PASCAL VOC, W: WATERCOLOR2K, B: BDD100K, CL: CLIPART. THE PROPOSED SF-DACA IS THE ONLY DATA AUGMENTATION-DRIVEN APPROACH IN THE SF-UDA SETTING SO FAR.

Method	Setting	In a nutshell	Base detector	Source \rightarrow Target	Code
ConfMix [30]	UDA	Self-training Cross-domain image mixing	YOLOv5	C \rightarrow F, S \rightarrow C K \rightarrow C	link
DACA [31]	UDA	Self-training Target-only region mixing Data augmentation	YOLOv5	C \rightarrow F S \rightarrow C K \rightarrow C	link
DA-Detect [24]	UDA	Image-level and object-level adaptation Adversarial mining for hard examples Auxiliary domain generation	Faster R-CNN	C \rightarrow F C \rightarrow K	link
SC-UDA [52]	UDA	Intermediate domain generation with optimized CycleGAN Iterative self-training Uncertainty-based pseudo-label optimization	Faster R-CNN	C \rightarrow F S \rightarrow C K \rightarrow C	\times
ViSGA [37]	UDA	Instance-level feature aggregation Similarity-based RPN proposal clustering Alignment via adversarial training	Faster R-CNN	C \rightarrow F S \rightarrow C K \rightarrow C	\times
SOAP [50]	SF-UDA	Mean teacher Perturbed target images	Faster R-CNN	C \rightarrow F, S \rightarrow C K \rightarrow C, P \rightarrow W	link
SFOD-Mosaic [26]	SF-UDA	Mining pseudo-label threshold via self-entropy descent	Faster R-CNN	C \rightarrow F, S \rightarrow C K \rightarrow C, C \rightarrow B	\times
LODS [25]	SF-UDA	Mean teacher Non-linear target style enhancement	Faster R-CNN	C \rightarrow F, K \rightarrow C P \rightarrow Cl, P \rightarrow W	link
ASFOD [5]	SF-UDA	Student-teacher Adversarial learning Source-similarity-based target division	Faster R-CNN	C \rightarrow F, S \rightarrow C K \rightarrow C, C \rightarrow B	link
LPU [4]	SF-UDA	Mean teacher Confident pseudo-labels Proposal soft training on low-confident pseudo-detections	Faster R-CNN	C \rightarrow F, S \rightarrow C K \rightarrow C, C \rightarrow B	\times
SF-UT [14]	SF-UDA	Mean teacher Adaptive Batch Normalization	Faster R-CNN	C \rightarrow F, S \rightarrow C K \rightarrow C	link
SF-DACA (ours)	SF-UDA	Mean teacher Target-only region mixing Data augmentation	Faster R-CNN	C \rightarrow F S \rightarrow C K \rightarrow C	Soon

image region, we calculate the average detection confidence of all the detections whose bounding box centers fall into it, and we retain only the most confident region r_{conf} with the highest average detection confidence, as in Eq. 1, along with its pseudo-labels,

$$r_{conf} = \{r : r \in (r_{tl}, r_{tr}, r_{bl}, r_{br}) \text{ if } p_r = \max(P_{stu})\}, \quad (1)$$

where $P_{stu} = (\bar{p}_{tl}, \bar{p}_{tr}, \bar{p}_{bl}, \bar{p}_{br})$ stands for the region-wise average detection confidences.

Second, to create challenging samples for the detector to learn from, the confident image region r_{conf} and its respective detections are augmented randomly four times (see Fig. 1), and the augmented versions of that region are joined into a single composite image,

$$x_{comp}, b_{comp}, c_{comp} = \cup_{i=1}^4 S_i(r_{conf}, b_{conf}, c_{conf}), \quad (2)$$

where S_i is the random augmentations function, x_{comp} is the composed challenging target image, b_{comp} is the set of augmented bounding boxes and c_{comp} is the set of classes, b_{conf} and c_{conf} are the set of bounding boxes of the confident target region and their object classes respectively.

Afterwards, the composite image x_{comp} is fed to the student model for inference, and the consistency loss ℓ_s between the inferred detections $y_{inf} = (b_{inf} \in \mathbb{R}^{M_{inf} \times 4}, c_{inf} \in \mathbb{N}^{M_{inf} \times 1})$ and the composite detections $y_{comp} = (b_{comp} \in \mathbb{R}^{M_{comp} \times 4}, c_{comp} \in \mathbb{N}^{M_{comp} \times 1})$ is calculated,

$$\ell_s = \mathcal{L}(y_{comp}, y_{inf}), \quad (3)$$

where $\mathcal{L}(\cdot)$ is the loss function of the adopted detection model.

C. Adaptation

The adaptation process of the student model Θ_{stu} follows a selective augmentation approach of image regions and their pseudo-detections. Ideally, these regions should comprise only true positives. However, this does not hold as image regions entail outlier false positives as well. The augmentation step further accumulates the contribution of these outliers, leading the detector to collapse eventually. Moreover, the knowledge of the student model gained on the source domain in the pretraining phase is prone to be forgotten.

To cope with this bottleneck, we back up the adaptation process with another teacher model Θ_{tea} also pretrained on

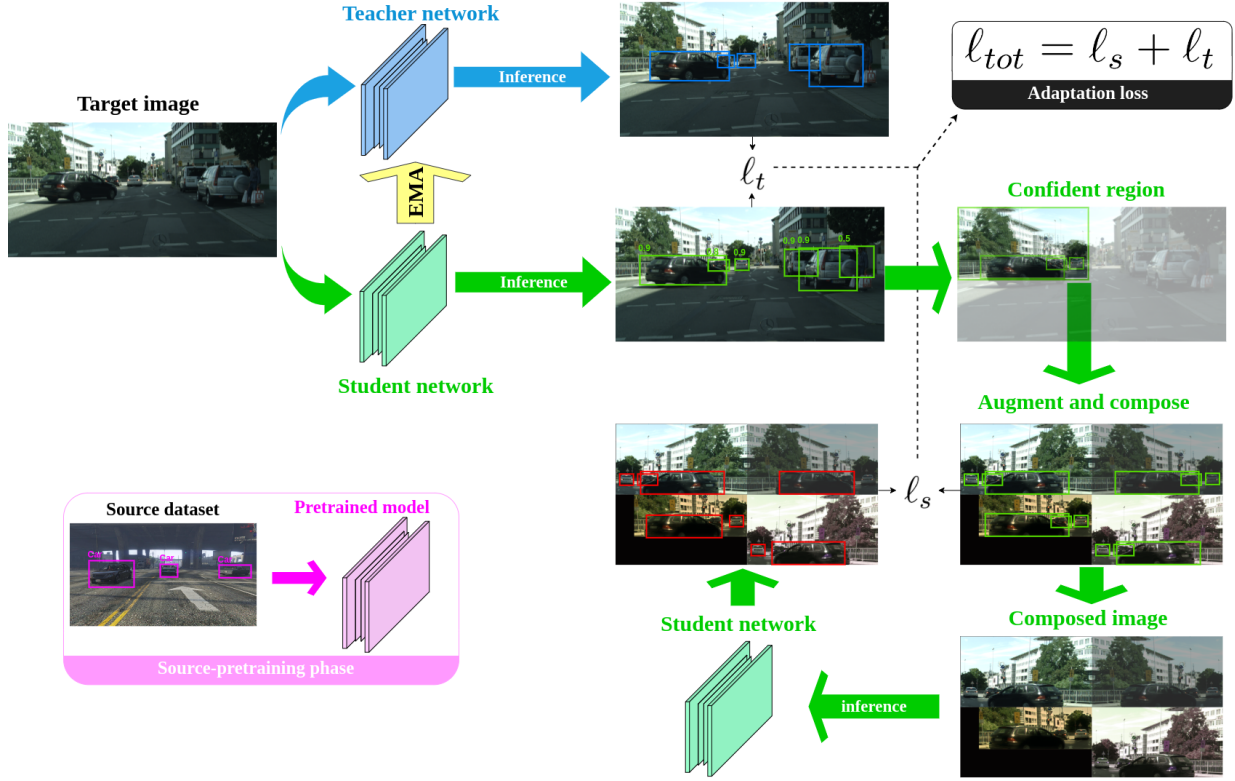


Fig. 1. Proposed SF-DACA. The student and the teacher models possess the same source-pretrained architecture (bottom-left). The green flow indicates adaptation towards the target via self-training with augmented and composed confident target regions. The blue flow refers to the teacher supervision to refrain the student from collapsing. Yellow flow ensures that the teacher model distills target knowledge from the student progressively along the adaptation progress.

the source data. Although source data is inaccessible, the source-pretrained model does convey rich information about the source domain. As depicted in Fig. 1, the target image x_t is fed to both the student and teacher models. The teacher receives the whole target image and delivers M_{tea} pseudo-labels $y_{tea} = (b_{tea} \in \mathbb{R}^{M_{tea} \times 4}, c_{tea} \in \mathbb{N}^{M_{tea} \times 1}, p_{tea} \in \mathbb{R}^{M_{tea} \times 1})$, where p_{tea} is the detection confidence. Simultaneously, as described previously, the student receives the whole target image and discerns M_{stu} pseudo-labels $y_{stu} = (b_{stu} \in \mathbb{R}^{M_{stu} \times 4}, c_{stu} \in \mathbb{N}^{M_{stu} \times 1}, p_{stu} \in \mathbb{R}^{M_{stu} \times 1})$. The consistency loss can then be calculated as in Eq. 4. Finally, the total adaptation loss ℓ_{tot} is given in Eq. 5.

$$\ell_t = \mathcal{L}(y_{tea}, y_{stu}), \quad (4)$$

$$\ell_{tot} = \ell_s + \ell_t. \quad (5)$$

The student model is supervised with ℓ_s to approach the target domain, and distills knowledge from the teacher model via ℓ_t to prevent catastrophic forgetting. To controllably progress the knowledge of the teacher model towards the target, we adopt an exponential moving average (EMA) [48] to pass knowledge from the student to the teacher by partially sharing its parameters,

$$\theta_{tea} = \alpha \cdot \theta_{tea} + (1 - \alpha) \cdot \theta_{stu}, \quad (6)$$

where α is a hyperparameter that controls the amount of student parameters that are shared to the teacher. This step is invoked at the end of each adaptation epoch as detailed in Pseudocode 1.

Algorithm 1: Pseudocode of SF-DACA.

input : θ_{stu} and θ_{tea} , target images x_t^i , random augmentations S , loss function $\mathcal{L}(\cdot)$, epochs N_{ep} , iterations N_{it} .
output: Adapted model θ_{stu} .

```

1 for  $ep = 1, \dots, N_{ep}$  do
2   for  $i = 1, \dots, N_{it}$  do
3     Feed  $x_t^i$  to  $\theta_{stu}$  and obtain  $y_{stu}$ ,
4     Divide the image equally into 2x2 layout,
5     Select  $r_{conf}$  (Eq. 1),
6     Augment and compose (Eq. 2),
7     Feed  $x_{comp}$  to  $\theta_{stu}$  and obtain  $y_{inf}$ ,
8     Compute  $\ell_s \leftarrow \mathcal{L}(y_{comp}, y_{inf})$ ,
9     Feed  $x_t^i$  to  $\theta_{tea}$  and obtain  $y_{tea}$ ,
10    Compute  $\ell_t \leftarrow \mathcal{L}(y_{tea}, y_{stu})$ ,
11    Compute and minimize  $\ell_{tot} = \ell_s + \ell_t$ ,
12  end
13  Update teacher with EMA:
14     $\theta_{tea} \leftarrow \alpha \cdot \theta_{tea} + (1 - \alpha) \cdot \theta_{stu}$ ,
15 end

```

IV. EXPERIMENTS

A. Datasets

We validated SF-DACA on four traffic scenes datasets: Cityscapes [6], FoggyCityscapes [42], Sim10K [19], and

KITTI [10]. Cityscapes (C) comprises real-world urban scenes captured across different cities. It includes object bounding box annotations for eight categories: Person, Rider, Car, Truck, Bus, Train, Motorcycle, and Bicycle. FoggyCityscapes (F) is a modified version of Cityscapes, generated by applying a synthetic fog filter to the original Cityscapes images. Sim10K (S) consists of synthetic images generated with the GTA-V game engine. KITTI (K) is a real-world traffic scenes dataset. To be consistent with previous SF-UDA works [50], [26], [25], [5], [4], [14], we considered three adaptation scenarios. The first one, denoted as $C \rightarrow F$, considers Cityscapes as the source domain and FoggyCityscapes as the target domain, addressing the adaptation to different weather conditions (clear vs foggy). It encompasses eight object categories. The second one, $K \rightarrow C$, involves cross-camera adaptation for the Car category, with KITTI as the source and Cityscapes as the target. The third scenario, $S \rightarrow C$, focuses on synthetic-to-real adaptation for the Car category, using Sim10K as the source domain and Cityscapes as the target.

B. Implementation details

For the sake of fairness with existing SF-UDA approaches, we consider Faster R-CNN [36] with a VGG16 backbone pretrained on ImageNet [45] as the base detector. The images are resized such that the shorter size is set to 600 pixels.

As optimizer, we opt for stochastic gradient descent with a learning rate of $1e-3$ and a momentum of 0.9. In the pretraining phase, the model is trained for 5 epochs on the Cityscapes dataset when dealing with the $C \rightarrow F$ scenario, for 1 epoch on KITTI and Sim10K regarding $K \rightarrow C$ and $S \rightarrow C$, respectively. As per the adaptation phase, the detector is trained for 12 epochs for all three scenarios. The layout of 2×2 is considered to build the composite target image according to our findings in our previous work [31]. This entails that the most confident region of the target image is augmented 4 times randomly, and the 4 augmented versions are put together into a 2×2 layout to form an image as shown at the bottom right of Fig. 1. An ablation on the most effective combination of data augmentations can be found in [31]. The mean average precision (mAP) and the average precision (AP) with an IoU threshold of 0.5 are reported as evaluation metrics.

C. Results and discussion

Tables II and III present quantitative results comparing SF-DACA with several source-free competitors based on the same detector and backbone, to ensure fairness. Specifically, we compare against SF-UT [14], LPU [4], ASFOD [5], LODS [25], SFOD [26], and SOAP [50]. The Source and Oracle notations (rows 1 and 2 in the tables) denote the cases when the detector is trained only on the source data, and only on the target data, indicating the lower bound when the model is not adapted and the upper bound based on target groundtruth.

The results of the $C \rightarrow F$ adaptation scenario are summarized in Tab. II. Compared to the Source baselines, our method achieves a 9.50% mAP gain (row 10 in the table). Bicycle is the category that achieves the most gain w.r.t the source-only model, and Bus yields the lowest improvement. On the

other hand, Bicycle and Rider classes are only 1.30% and 1.50% mAP away from the Oracle performance, and Bus class remains the least adaptable class among all (-19.00% mAP loss w.r.t the Oracle), followed by the Train class (-13.90%). Interestingly, the Train category reports a very low score (1.70%) based on the source-only model. This implies that the adaptation starts with a model that possesses marginal knowledge about this class, posing self-adaptation issues. Note that this is the most difficult adaptation scenario due to the foggy weather and the multiple classes encountered in urban scenes. Compared with prior works, our method ranks third respectively after SF-UT [14] and LPU [4] mainly due to the low scores observed for the Bus and Train classes. By contrast, on the Car, Rider and Person categories, our method ranks first with improvements of 3.00%, 3.20% and 1.00% compared with SF-UT [14].

Concerning the $K \rightarrow C$, and $S \rightarrow C$ adaptation cases, the scores are given in Tab. III. Remarkable improvements (+18.20% and +22.90%) are incurred for $K \rightarrow C$ and $S \rightarrow C$, respectively. Compared to the state-of-the-art, for the $K \rightarrow C$ our method ranks first among all with a large margin, followed by LPU [4] then SF-UT [14]. As per $S \rightarrow C$, our method ranks first, followed by SF-UT [14] then LPU [4]. Although the synthetic-to-real ($S \rightarrow C$) scenario starts from a lower score (36.70%) compared to the cross-camera case ($K \rightarrow C$, with 38.60%), its score post adaptation is higher (59.60% vs 56.80%), suggesting that domain discrepancy is larger in the cross-camera adaptation. Note that the adaptation gain in these two benchmarks remains much higher than the Car class of the $C \rightarrow F$ (18.20% and 22.90% vs 10.60%) mainly due to the severe domain shift in this latter case.

Qualitative examples before and after adaptation are illustrated in Fig. 2, for $C \rightarrow F$, $K \rightarrow C$ and $S \rightarrow C$ scenarios respectively, where less false positives, more true positives, and better fitted bounding boxes and higher confidences are observed post adaptation with SF-DACA.

D. Ablation study

Pseudo-label selection confidence. Prior to selecting the most confident region with the highest confidence, all the detections inferred in the image undergo a selection step to filter out the likely false positives. This is done by simply imposing a selection confidence threshold. We report the adaptation scores for all the three adaptation cases in Tab. IV according to different pseudo-label selection confidence values. In particular, in the $C \rightarrow F$ case, the mAP improves as the confidence increases up to a confidence threshold of 0.5, exhibiting a downward trend afterwards. This suggests that pseudo-labels with low confidence below the value of 0.5 contain many false positives that misguide the adaptation. Increasing the confidence beyond the value of 0.5 results in confident detections but at the cost of less true positives that are useful for the adaptation. Thus, we opt for a trade-off threshold of 0.5 as default choice.

Regarding the $K \rightarrow C$ and the $S \rightarrow C$ scenarios, the adaptation score manifests an upward trend along with the pseudo-label confidence. This is traced back to the fact these two benchmarks envision a one class adaptation problem, whereas in the earlier $C \rightarrow F$ benchmark, the studied threshold is imposed on



Fig. 2. Qualitative examples from the C→F (top 2 rows), K→C (middle 2 rows) and S→C (bottom 2 rows) adaptation scenarios. Detections of source-pretrained model (left) versus predictions of target-adapted model via SF-DACA (right). Green bounding boxes refer to the groundtruth, and red ones refer to the detections. Detected object class and confidence are provided on the top left of each instance. Best viewed in color.

TABLE II

RESULTS ON THE CITYSCAPES TO FOGGYCITYSCAPES ADAPTATION SCENARIO (C→F). ‘‘SOURCE ONLY’’ (ROW 1) REFERS TO THE LOWERBOUND SCORES OBTAINED BY THE SOURCE-PRETRAINED MODEL PRIOR TO ADAPTATION. ‘‘ORACLE’’ (ROW 2) INDICATES THE UPPERBOUND SCORES BY TRAINING THE MODEL ON THE TARGET GROUNDTRUTH. ROW 10 REPORTS THE GAIN W.R.T THE SOURCE-ONLY (ROW 1). BEST PERFORMANCES ARE HIGHLIGHTED IN BOLD.

	Method	Person	Car	Train	Rider	Truck	Motorcycle	Bicycle	Bus	mAP
1	Source-only	35.20	51.30	1.70	41.90	12.90	18.70	29.40	32.20	27.90
2	Oracle	48.60	67.10	25.80	52.70	35.10	38.80	44.90	53.70	45.90
3	SOAP [50]	35.90	48.40	24.30	45.00	23.90	31.80	37.90	37.20	35.50
4	SFOD [26]	33.20	44.50	22.20	40.70	25.50	28.40	34.10	39.00	33.50
5	LODS [25]	34.00	48.80	19.60	45.70	27.30	33.20	37.80	39.70	35.80
6	ASFOD [5]	32.30	44.60	29.00	44.10	28.10	31.80	38.90	34.30	35.40
7	LPU [4]	39.00	55.40	21.20	50.30	24.00	30.30	44.20	46.00	38.80
8	SF-UT [14]	40.90	58.90	50.20	48.00	29.60	36.20	44.10	51.90	45.00
9	SF-DACA (ours)	41.90	61.90	11.90	51.20	24.80	29.00	43.60	34.70	37.40
10	Gain w.r.t. row 1	+6.70	+10.60	+10.20	+9.30	+11.90	+10.30	+14.20	+2.50	+9.50

TABLE III

RESULTS ON THE KITTI TO CITYSCAPES (K→C) AND THE SIM10K TO CITYSCAPES (S→C) ADAPTATION SCENARIOS. SOURCE (ROW 1) REFERS TO THE LOWERBOUND SCORES OBTAINED BY THE SOURCE-PRETRAINED MODEL PRIOR TO ADAPTATION. ORACLE (ROW 2) INDICATES THE UPPERBOUND SCORES BY TRAINING THE MODEL ON THE TARGET GROUNDTRUTH. ROW 10 REPORTS THE GAIN W.R.T THE SOURCE-ONLY (ROW 1). BEST PERFORMANCES ARE HIGHLIGHTED IN BOLD.

	Method	K→C	S→C
1	Source only	38.60	36.70
2	Oracle	67.70	67.70
3	SOAP [50]	41.90	40.80
4	SFOD [26]	44.60	43.10
5	LODS [25]	43.90	-
6	ASFOD [5]	44.90	44.00
7	LPU [4]	48.40	47.30
8	SF-UT [14]	46.20	55.40
9	SF-DACA (ours)	56.80	59.60
10	Gain w.r.t. row 1	+18.20	+22.90

TABLE IV

EFFECT OF THE PSEUDO-LABEL SELECTION CONFIDENCE.

	Selection conf.	C→F	K→C	S→C
1	0.10	16.50	34.70	27.60
2	0.30	31.30	41.30	42.20
3	0.50	36.10	45.60	48.40
4	0.70	35.70	46.90	50.50
5	0.90	32.60	54.30	57.30
6	0.95	32.30	56.80	59.60

all the eight object classes. Therefore, for these two scenarios, the default threshold is set to 0.95.

Amount of shared student knowledge. Note that the scores reported in the previous ablations were conducted with an EMA coefficient (Eq. 6) of 0.9. Here, we fix the detection confidence according to the best values obtained earlier for each scenario and we further study the effect of α on the results as given in Tab. V for all the three benchmarks. In all scenarios, the behaviors are about the same, where the performance increases as the α value is raised, up to a certain point (α of 0.95 in the C→F benchmark and 0.9 otherwise) where it starts to decline afterwards. This suggests that sharing too much knowledge from the student to the teacher (i.e., small α) leads the teacher to lose its own prior knowledge,

TABLE V

EFFECT OF THE AMOUNT OF SHARED KNOWLEDGE FROM THE STUDENT MODEL TO THE TEACHER MODEL.

	α	C→F	K→C	S→C
1	0.30	23.10	42.50	51.10
2	0.50	26.40	46.10	53.40
3	0.70	30.50	48.00	54.60
4	0.80	33.40	52.60	57.30
5	0.90	36.10	56.80	59.60
6	0.95	37.40	56.30	57.30
7	0.99	35.90	55.10	57.70

causing the student to learn improperly from the teacher. By contrast, sharing a small amount of weights from the student to the teacher (i.e., large α) causes the teacher to stagnate and holds the student from progressing its knowledge towards the target domain. Therefore, default values of 0.95 for the C→F scenario and 0.9 otherwise are adopted.

Does the teacher matter? As explained before, the teacher model is employed to prevent the student model from collapsing during adaptation. To highlight this, we conduct the adaptation experiments on the three adaptation benchmarks by dropping the teacher model and letting the student learn on its own. We report the mAP at each adaptation iteration as depicted in Fig. 3. The effect of the teacher model is evident as the student phases out and fails to maintain a stable trend. In particular, the performance starts from the source-pretrained mAPs reported in Tab. II and Tab. III and flattens after a couple of hundreds of iterations (i.e., note that an adaptation epoch is worth approximately 3000 iterations, yet the performance vanishes in far less than one epoch).

Does DACA matter? Earlier, we studied the impact when the teacher model is discarded, causing a premature performance slope. Here, we study the impact when the DACA part is dropped (i.e., Eq. 5 relaxed to $l_{tot} = l_s$) leaving only the teacher model to self-adapt. We report the results in Tab. VI for all the three scenarios. While in the K→C and the S→C cases, the improvements of introducing DACA amount to 1.50% and 1.30% respectively, in the C→F benchmark the gain reaches 3.20%. This stresses the role of DACA, especially when the domain gap is severe as in C→F.

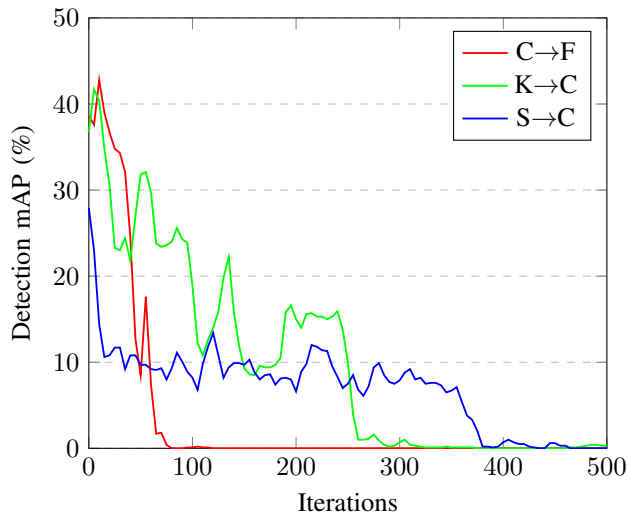


Fig. 3. Effect of catastrophic forgetting phenomenon when the teacher model is discarded. Best viewed in color.

TABLE VI
IMPORTANCE OF DACA IN THE ADAPTATION PROCESS.

Scenario	C→F	K→C	S→C
1 Without DACA	34.20	55.30	58.30
2 With DACA	37.40	56.80	59.60
3 Improvement	+3.20	+1.50	+1.30

V. CONCLUSIONS

Data augmentation is useful to create informative samples to train object detection models, especially when the annotations are unavailable as in the task of source-free domain adaptation. However, no work has attempted to tailor it so far. This paper proposed a novel source-free domain adaptation scheme for object detection. It makes use of data augmentation by mining image regions and their respective confident pseudo-labels and reproducing them into challenging composite images that are leveraged to adapt a detector via self-training. The method was tested on three adaptation benchmarks, scoring new state-of-the-art on two of them.

Limitations. Our method augments image regions along with their detections, which may contain false positives that are also augmented, misleading the adaptation of the detector.

Future work. To help eliminate false positives and alleviate their contribution in the adaptation process, we believe that zero shot models [27] can be explored to extract high quality pseudo-labels prior to adaptation with SF-DACA.

REFERENCES

- [1] Everton L Aleixo, Juan G Colonna, Marco Cristo, and Everlandio Fernandes. Catastrophic forgetting in deep learning: A comprehensive taxonomy. *arXiv preprint arXiv:2312.10549*, 2023.
- [2] Brais Bosquet, Daniel Cores, Lorenzo Seidenari, Víctor M Brea, Manuel Mucientes, and Alberto Del Bimbo. A full data augmentation pipeline for small object detection based on generative adversarial networks. *Pattern Recognition*, 133:108998, 2023.
- [3] Nicolas Carion, Francisco Massa, Gabriel Synnaeve, Nicolas Usunier, Alexander Kirillov, and Sergey Zagoruyko. End-to-end object detection with transformers. In *European conference on computer vision*, pages 213–229. Springer, 2020.

- [4] Zhihong Chen, Zilei Wang, and Yixin Zhang. Exploiting low-confidence pseudo-labels for source-free object detection. In *Proceedings of the 31st ACM International Conference on Multimedia*, pages 5370–5379, 2023.
- [5] Qiaosong Chu, Shuyan Li, Guangyi Chen, Kai Li, and Xiu Li. Adversarial alignment for source free object detection. In *Proceedings of the AAAI Conference on Artificial Intelligence*, pages 452–460, 2023.
- [6] M. Cordts, M. Omran, S. Ramos, T. Rehfeld, M. Enzweiler, R. Benenson, U. Franke, S. Roth, and B. Schiele. The Cityscapes dataset for semantic urban scene understanding. In *CVPR*, 2016.
- [7] Tausif Diwan, G Anirudh, and Jitendra V Tembhurne. Object detection using yolo: Challenges, architectural successors, datasets and applications. *multimedia Tools and Applications*, 82(6):9243–9275, 2023.
- [8] Haoyang Fang, Boran Han, Shuai Zhang, Su Zhou, Cuixiong Hu, and Wen-Ming Ye. Data augmentation for object detection via controllable diffusion models. In *Proceedings of the IEEE/CVF Winter Conference on Applications of Computer Vision*, pages 1257–1266, 2024.
- [9] Di Feng, Ali Harakeh, Steven L Waslander, and Klaus Dietmayer. A review and comparative study on probabilistic object detection in autonomous driving. *IEEE Transactions on Intelligent Transportation Systems*, 23(8):9961–9980, 2021.
- [10] Andreas Geiger, Philip Lenz, Christoph Stiller, and Raquel Urtasun. Vision meets robotics: The kitti dataset. *The International Journal of Robotics Research*, 32(11):1231–1237, 2013.
- [11] R Girshick. Fast r-cnn. *arXiv preprint arXiv:1504.08083*, 2015.
- [12] Ross Girshick, Jeff Donahue, Trevor Darrell, and Jitendra Malik. Rich feature hierarchies for accurate object detection and semantic segmentation. In *Proceedings of the IEEE conference on computer vision and pattern recognition*, pages 580–587, 2014.
- [13] Evgin Goceri. Medical image data augmentation: techniques, comparisons and interpretations. *Artificial Intelligence Review*, 56(11):12561–12605, 2023.
- [14] Yan Hao, Florent Forest, and Olga Fink. Simplifying source-free domain adaptation for object detection: Effective self-training strategies and performance insights. In *European Conference on Computer Vision*, pages 196–213. Springer, 2025.
- [15] Danfeng Hong, Bing Zhang, Hao Li, Yuxuan Li, Jing Yao, Chenyu Li, Martin Werner, Jocelyn Chanussot, Alexander Zipf, and Xiao Xiang Zhu. Cross-city matters: A multimodal remote sensing benchmark dataset for cross-city semantic segmentation using high-resolution domain adaptation networks. *Remote Sensing of Environment*, 299:113856, 2023.
- [16] Cheng-Chun Hsu, Yi-Hsuan Tsai, Yen-Yu Lin, and Ming-Hsuan Yang. Every pixel matters: Center-aware feature alignment for domain adaptive object detector. In *Computer Vision—ECCV 2020: 16th European Conference, Glasgow, UK, August 23–28, 2020, Proceedings, Part IX 16*, pages 733–748. Springer, 2020.
- [17] Han-Kai Hsu, Chun-Han Yao, Yi-Hsuan Tsai, Wei-Chih Hung, Hung-Yu Tseng, Maneesh Singh, and Ming-Hsuan Yang. Progressive domain adaptation for object detection. In *Proceedings of the IEEE/CVF winter conference on applications of computer vision*, pages 749–757, 2020.
- [18] Xun Huang and Serge Belongie. Arbitrary style transfer in real-time with adaptive instance normalization. In *Proceedings of the IEEE international conference on computer vision*, pages 1501–1510, 2017.
- [19] M. Johnson-Roberson, C. Barto, R. Mehta, S. N. Sridhar, K. Rosaen, and R. Vasudevan. Driving in the matrix: Can virtual worlds replace human-generated annotations for real world tasks? In *ICRA*, 2017.
- [20] Padmavathi Kora, Chui Ping Ooi, Oliver Faust, U Raghavendra, Anjan Gudigar, Wai Yee Chan, K Meenakshi, K Swaraja, Pawel Plawiak, and U Rajendra Acharya. Transfer learning techniques for medical image analysis: A review. *Biocybernetics and Biomedical Engineering*, 42(1):79–107, 2022.
- [21] Alex Krizhevsky, Ilya Sutskever, and Geoffrey E Hinton. Imagenet classification with deep convolutional neural networks. *Advances in neural information processing systems*, 25, 2012.
- [22] Teerath Kumar, Rob Brennan, Alessandra Mileo, and Malika Bendeche. Image data augmentation approaches: A comprehensive survey and future directions. *IEEE Access*, 2024.
- [23] Attila Lengyel, Sourav Garg, Michael Milford, and Jan C van Gemert. Zero-shot day-night domain adaptation with a physics prior. In *Proceedings of the IEEE/CVF International Conference on Computer Vision*, pages 4399–4409, 2021.
- [24] Jinlong Li, Runsheng Xu, Jin Ma, Qin Zou, Jiaqi Ma, and Hongkai Yu. Domain adaptive object detection for autonomous driving under foggy weather. In *Proceedings of the IEEE/CVF Winter Conference on Applications of Computer Vision*, pages 612–622, 2023.
- [25] Shuai Feng Li, Mao Ye, Xi Tian Zhu, Lihua Zhou, and Lin Xiong. Source-free object detection by learning to overlook domain style. In

- Proceedings of the IEEE/CVF Conference on Computer Vision and Pattern Recognition*, pages 8014–8023, 2022.
- [26] Xianfeng Li, Weijie Chen, Di Xie, Shicai Yang, Peng Yuan, Shiliang Pu, and Yueting Zhuang. A free lunch for unsupervised domain adaptive object detection without source data. In *Proceedings of the AAAI Conference on Artificial Intelligence*, pages 8474–8481, 2021.
- [27] Shilong Liu, Zhaoyang Zeng, Tianhe Ren, Feng Li, Hao Zhang, Jie Yang, Qing Jiang, Chunyuan Li, Jianwei Yang, Hang Su, et al. Grounding dino: Marrying dino with grounded pre-training for open-set object detection. In *European Conference on Computer Vision*, pages 38–55. Springer, 2025.
- [28] Wei Liu, Dragomir Anguelov, Dumitru Erhan, Christian Szegedy, Scott Reed, Cheng-Yang Fu, and Alexander C Berg. Ssd: Single shot multibox detector. In *Computer Vision—ECCV 2016: 14th European Conference, Amsterdam, The Netherlands, October 11–14, 2016, Proceedings, Part I 14*, pages 21–37. Springer, 2016.
- [29] Yan-Feng Lu, Jing-Wen Gao, Qian Yu, Yi Li, Yi-Sheng Lv, and Hong Qiao. A cross-scale and illumination invariance-based model for robust object detection in traffic surveillance scenarios. *IEEE Transactions on Intelligent Transportation Systems*, 2023.
- [30] Giulio Mattolin, Luca Zanella, Elisa Ricci, and Yiming Wang. Confmix: Unsupervised domain adaptation for object detection via confidence-based mixing. In *Proceedings of the IEEE/CVF Winter Conference on Applications of Computer Vision*, pages 423–433, 2023.
- [31] Mohamed Lamine Mekhalif, Davide Boscaini, and Fabio Poiesi. Detect, Augment, Compose, and Adapt: Four Steps for Unsupervised Domain Adaptation in Object Detection. In *The 34th British Machine Vision Conference*, 2023.
- [32] Farzeen Munir, Shoaib Azam, Muhammad Aasim Rafique, Ahmad Muqem Sheri, and Moongu Jeon. Thermal object detection using domain adaptation through style consistency. *arXiv preprint arXiv:2006.00821*, 4:12–13, 2020.
- [33] Poojan Oza, Vishwanath A Sindagi, Vibashan Vishnukumar Sharmini, and Vishal M Patel. Unsupervised domain adaptation of object detectors: A survey. *IEEE Transactions on Pattern Analysis and Machine Intelligence*, 2023.
- [34] Arun V Reddy, Ketul Shah, William Paul, Rohita Mocharla, Judy Hoffman, Kapil D Katyal, Dinesh Manocha, Celso M de Melo, and Rama Chellappa. Synthetic-to-real domain adaptation for action recognition: A dataset and baseline performances. *arXiv preprint arXiv:2303.10280*, 2023.
- [35] J Redmon. You only look once: Unified, real-time object detection. In *Proceedings of the IEEE conference on computer vision and pattern recognition*, 2016.
- [36] Shaoqing Ren, Kaiming He, Ross Girshick, and Jian Sun. Faster r-cnn: Towards real-time object detection with region proposal networks. *IEEE transactions on pattern analysis and machine intelligence*, 39(6):1137–1149, 2016.
- [37] Farzaneh Rezaeianaran, Rakshith Shetty, Rahaf Aljundi, Daniel Olmeda Reino, Shanshan Zhang, and Bernt Schiele. Seeking similarities over differences: Similarity-based domain alignment for adaptive object detection. In *Proceedings of the IEEE/CVF International Conference on Computer Vision*, pages 9204–9213, 2021.
- [38] Adrian Lopez Rodriguez and Krystian Mikolajczyk. Domain adaptation for object detection via style consistency. *arXiv preprint arXiv:1911.10033*, 2019.
- [39] T-YLPG Ross and GKHP Dollár. Focal loss for dense object detection. In *proceedings of the IEEE conference on computer vision and pattern recognition*, pages 2980–2988, 2017.
- [40] Arunabha M Roy, Rikhi Bose, and Jayabrata Bhaduri. A fast accurate fine-grain object detection model based on yolov4 deep neural network. *Neural Computing and Applications*, pages 1–27, 2022.
- [41] Aruni RoyChowdhury, Prithvijit Chakrabarty, Ashish Singh, SouYoung Jin, Huaizu Jiang, Liangliang Cao, and Erik Learned-Miller. Automatic adaptation of object detectors to new domains using self-training. In *Proceedings of the IEEE/CVF Conference on Computer Vision and Pattern Recognition*, pages 780–790, 2019.
- [42] Christos Sakaridis, Dengxin Dai, and Luc Van Gool. Semantic foggy scene understanding with synthetic data. *International Journal of Computer Vision*, 126:973–992, 2018.
- [43] Ranjan Sapkota, Rizwan Qureshi, Marco Flores-Calero, Chetan Badgular, Upesh Nepal, Alwin Poullose, Peter Zeno, Uday Bhanu Prakash Vaddevolu, Prof Yan, Manoj Karkee, et al. Yolov10 to its genesis: A decadal and comprehensive review of the you only look once series. *Available at SSRN 4874098*, 2024.
- [44] Fengyi Shen, Li Zhou, Kagan Kucukaytekin, Ziyuan Liu, He Wang, and Alois Knoll. Controluda: Controllable diffusion-assisted unsupervised domain adaptation for cross-weather semantic segmentation. *arXiv preprint arXiv:2402.06446*, 2024.
- [45] Karen Simonyan and Andrew Zisserman. Very deep convolutional networks for large-scale image recognition. *arXiv preprint arXiv:1409.1556*, 2014.
- [46] Petru Soviany, Radu Tudor Ionescu, Paolo Rota, and Nicu Sebe. Curriculum self-paced learning for cross-domain object detection. *Computer Vision and Image Understanding*, 204:103166, 2021.
- [47] Mingxing Tan, Ruoming Pang, and Quoc V Le. Efficientdet: Scalable and efficient object detection. In *Proceedings of the IEEE/CVF conference on computer vision and pattern recognition*, pages 10781–10790, 2020.
- [48] Antti Tarvainen and Harri Valpola. Mean teachers are better role models: Weight-averaged consistency targets improve semi-supervised deep learning results. *Advances in neural information processing systems*, 30, 2017.
- [49] Berkcan Ustun, Ahmet Kagan Kaya, Ezgi Cakir Ayerden, and Fazil Altinel. Spectral transfer guided active domain adaptation for thermal imagery. In *Proceedings of the IEEE/CVF Conference on Computer Vision and Pattern Recognition*, pages 449–458, 2023.
- [50] Lin Xiong, Mao Ye, Dan Zhang, Yan Gan, Xue Li, and Yingying Zhu. Source data-free domain adaptation of object detector through domain-specific perturbation. *International Journal of Intelligent Systems*, 36(8):3746–3766, 2021.
- [51] Mingle Xu, Sook Yoon, Alvaro Fuentes, and Dong Sun Park. A comprehensive survey of image augmentation techniques for deep learning. *Pattern Recognition*, 137:109347, 2023.
- [52] Fuxun Yu, Di Wang, Yinpeng Chen, Nikolaos Karianakis, Tong Shen, Pei Yu, Dimitrios Lymberopoulos, Sidi Lu, Weisong Shi, and Xiang Chen. Sc-uda: Style and content gaps aware unsupervised domain adaptation for object detection. In *Proceedings of the IEEE/CVF Winter Conference on Applications of Computer Vision*, pages 382–391, 2022.
- [53] Ruiheng Zhang, Lingxiang Wu, Yukun Yang, Wanneng Wu, Yueqiang Chen, and Min Xu. Multi-camera multi-player tracking with deep player identification in sports video. *Pattern Recognition*, 102:107260, 2020.
- [54] Huabing Zhou, Jiayi Ma, Chiu C Tan, Yanduo Zhang, and Haibin Ling. Cross-weather image alignment via latent generative model with intensity consistency. *IEEE transactions on image processing*, 29:5216–5228, 2020.
- [55] Huayi Zhou, Fei Jiang, and Hongtao Lu. Ssda-yolo: Semi-supervised domain adaptive yolo for cross-domain object detection. *Computer Vision and Image Understanding*, 229:103649, 2023.
- [56] Xingyi Zhou, Dequan Wang, and Philipp Krähenbühl. Objects as points. *arXiv preprint arXiv:1904.07850*, 2019.
- [57] Xinge Zhu, Jiangmiao Pang, Ceyuan Yang, Jianping Shi, and Dahua Lin. Adapting object detectors via selective cross-domain alignment. In *Proceedings of the IEEE/CVF Conference on Computer Vision and Pattern Recognition*, pages 687–696, 2019.
- [58] Zhuangdi Zhu, Kaixiang Lin, Anil K Jain, and Jiayu Zhou. Transfer learning in deep reinforcement learning: A survey. *IEEE Transactions on Pattern Analysis and Machine Intelligence*, 2023.
- [59] Zhengxia Zou, Keyan Chen, Zhenwei Shi, Yuhong Guo, and Jieping Ye. Object detection in 20 years: A survey. *Proceedings of the IEEE*, 111(3):257–276, 2023.